Indian Journal of Science and Technology, *Vol 8(23), DOI: 10.17485/ijst/2015/v8i23/73052, September 2015*
ISSN (Print) : 0974-6846
ISSN (Online) : 0974-5645

A Robust Edge Preserving Bilateral Filter for Ultrasound Kidney Image

T. Loganayagi[1]* and K. R. Kashwan[2]

[1]Department of ECE, Mahendra Engineering College, Namakkal - 637 503, Tamil Nadu, India; t.loganayagi@gmail.com
[2]Department of ECE, Sona College of Technology, Salem - 636 006, Tamil Nadu, India; kashwan.kr@gmail.com

Abstract

Objective: The speckle noise reduction is an important preprocessing step, normally performed to improve the segmentation of kidney images for the diagnosis of stones' presence or its size. The bilateral filter is a robust method for noise reduction with edge preservation. An attempt is made in this work to analyze the effectiveness of the bilateral filter for speckle reduction in ultrasound kidney images. **Methods/Statistical Analysis:** An open source software *Fiji*is used to develop the filtering algorithms for ultrasound kidney image. The bilateral filter performance is compared with familiar speckle filters named median filter, Speckle Reducing Anisotropic Diffusion (SRAD) filter and Non-Local Mean (NLM) filter. The authors have selected mainly Root Mean Square Error (RMSE) for image quality analysis, Signal to Noise Ratio (SNR) for comparison of noise with useful signal strength, Peak Signal to Noise Ratio (PSNR) for maximum amplitude of signal, Mean Absolute Error (MAE) for overall performance and Structural Similarity Index Measure (SSIM) for testing bilateral filter on kidney images. The statistical measures also calculated to distinguish the filter performances. **Findings:** The bilateral filter performance is proven as an effective method for speckle reduction in ultrasound kidney stone detection applications than the existing methods through quantitative and statistical analysis. **Application/Improvement:** The bilateral filter can offer better segmentation of kidney stone due to its effective speckle reduction.

Keywords: Bilateral Filtering, Despeckling, Edge Preservation, Fiji, Kidney Stone, Ultrasound Image

1. Introduction

Ultrasound imaging is a coherent system to acquire images of internal organs using the principles of ultrasound. The images so acquired help in diagnoses in medicine for many ailments and disorders of body organs including heart, blood vessels, liver, gall bladder, spleen, kidney, pancreas, uterus, ovaries, bladder, eyes, prostate etc. It also helps physicians to determine medical procedures to treat soft tissue injuries after locating the same.

Ultrasound imaging techniques are preferred over Computed Tomography (CT), Magnetic Resonance Imaging (MRI), etc. due to its non-invasive, radiation-free and cheaper existence. The problem with the ultrasound image is it poor quality due to the granular pattern called speckle[1]. Speckle noise can be represented by multiplicative noise model. It is caused if incident ultrasound waves back scatter towards the image acquiring sensor. The reflected waves with random phase angles can cause a granular noise in an acquired image due to interference with desired image signals. The speckle noise reduction, therefore, is critical for interpretation of possible diagnosing information available on ultrasound image. The low quality of the ultrasound image in the presence of speckle noise may be due to suppression of boundaries, missing edges and misrepresentation of spatial details. The edges

**Author for correspondence*

in image play the important role for segmentation of images. The speckle reduction may also lead to limit the contrast ratio, which in turn can hamper the performance of segmentation and classification algorithms which are normally applied on images.

The bilateral filter[2], developed by Tomasi C and Manduchi R, is a better choice for Gaussian noise as it preserves edges of an image. It is also suitable for removing speckle noise. The bilateral filter is applied for medical image processing for diagnosis different disorders[3]. The conventional architecture of bilateral filter is further improved[4,5] specifically for speckle noise in ultrasound images. The new architecture[5] reduces the speckle noise far more and outlines the region of interest better. A new multi-resolution concept is integrated with the bilateral filter using wavelets to improve the performance[6–8]. The bilateral filter is applied for edge detection and edge enhancement algorithms for color spaces with better results. An integration of bilateral filter, edge detection and edge enhancement based on color spaces is proposed[9] by Kao et al. This approach reduces the noise while preserving edges. The false edge detection is also reduced. This can improve the image. The integrated approach is suitable for textures, but the smoothing of the image is not improved. The findings by researchers suggest that a bilateral filter is suitable for all types of noises. Han et al. have embedded a novel interpolation framework[10] with bilateral filter to further improve denoising and sharpening of images.

The simulated results of the bilateral filter in this work are compared with existing speckle filters like median filter[11,12] anisotropic diffusion filter[12–15] and Nonlocal Mean Filter (NLM)[16,17]. Schindelin Jet al.[18] was used *Fiji* platform for medical image analysis. *Fiji* software also provides an opportunity to software engineering community for the biological imaging research, collaboration and exchange of knowledge. The *Fiji* software offers GUI and used for ultrasound kidney image processing in this work. The performance is analyzed through RMSE, PSNR and SSIM[19] and the filters are compared.

2. Materials and Methods

2.1 Speckle Filters

The speckle noise in the ultrasound image is undesirable. Several speckle filters[11,12] are used to reduce speckle noise. It depends upon signals and requires specific filter characteristics for speckle reduction. This section presents a few of often used speckle filters.

2.1.1 Median Filter

Median filter[11,12] reduces the speckle noise of ultrasound image by replacing each pixel with the median of neighborhood pixel values. A 3×3 window size is used for computing the median value of concern pixel.

2.1.2 Anisotropic Diffusion Filter

Anisotropic filtering[12,13] is a nonlinear method for improving contrast and speckle noise reduction simultaneously by varying coefficients. It is named as Speckle Reducing Anisotropic Filtering (SRAD) with extended application in the field of medical and radar imaging. This filter preserves prominent edges while reducing speckle noise by preventing diffusion across the edges and permitting diffusion on either side of the edges. The concept of SRAD[13] presented by Saini K et al. is used in this work for comparison with other filters.

2.1.3 Nonlocal Means Filter

The NLM filter[16,17] removes the noise in the image without affecting the details. It also provides clean edges. It uses the similarity existing in the image to evaluate the pixel weights by assuming that the image comprises a wide range of similarity itself. In denoising process, the averaging of pixels provides the denoised pixel similar to its original value. This is due to the more pixels correlation and identically independently distributed noise component. As noise increases the NLM algorithm fails to preserve edges and details in the image. The NLM filter[16] framework discussed by Buades A et al. is used in this work for comparing filter performances.

2.1.4 Bilateral Filter

The nonlinear and non-iterative bilateral filtering[2] concept was developed for edge preservation and smoothing of the noisy image. The bilateral filtering replaces a noisy pixel of an image by a weighted value depending on the geometric distance and photometric distance. Based on the choice of weighting functions, different types of bilateral filters are developed.

Let us consider a pixel location X which is center pixel in a given window and Y is any another pixel in the same window. Then the output of bilateral filter for speckle noise[4] is expected as

$$\tilde{I}(X)=\frac{1}{c}\sum Y\in N(X)e^{\frac{-\|Y-X\|}{2\sigma_d^2}}.e^{\frac{|I(Y)-I(X)|^2}{2\sigma_r^2}}.I(Y) \qquad (1)$$

Where, $\|Y-X\|$ is the Euclidean distance between two pixel X, Y and can be determined as

$$\|Y-X\| = \sqrt{X^2-Y^2} \qquad (2)$$

$$\tilde{I}(X)=\frac{1}{c}\sum Y\in N(X)e^{\frac{-(X^2-Y^2)}{2\sigma_d^2}}.e^{\frac{|I(Y)-I(X)|^2}{2\sigma_r^2}}.I(Y) \qquad (3)$$

Where C is normalization constant given by

$$C=\sum_{Y\in N(X)} e^{\frac{-(X^2+Y^2)}{2\sigma_d^2}}.e^{\frac{-|I(Y)-I(X)|^2}{2\sigma_r^2}} \qquad (4)$$

Here, *I(X)* is a center pixel in a given mask and *I(Y)* is any other pixel other than the center pixel in the given window. The function, $|Y-X|$ measures the spatial distance and $|I(Y)-I(X)|$ measures the distance between any two intensity values of pixels X and Y. The σ_d and σ_r are the geometric spread in domain filter part and photometric spread in range filter part, respectively[3]. The σ_d value σ_r decides the amount of low pass filtering and decides the amount of range filtering required. An image is scaled up or down by adjusting and amplified or attenuated by adjusting σ_r.

2.2 Bilateral Filter Implementation in FIJI

ImageJ is an open-source platform for biomedical image analysis. It is easy to use and can handle different image processing tasks. It is originally developed by a biologist with the lack of computer science principles. A new open source software *Fiji* is developed to address the deficiency of *ImageJ*. *Fiji* allows the researcher to apply innovative solutions for biomedical image analysis. With modern software engineering practice, *Fiji* has many library functions. It can be used easily for numerous algorithms to improve image processing. *Fiji* is used to analyze new algorithms for image analysis using its library functions. A set of *Fiji* plugin and library for medical image analysis is provided. The inbuilt plugin is a dedicated mechanism of image processing algorithms. The algorithms include third party libraries, user developed macros and scripts. The third party plugin libraries include Biomed group, ij plugin and Biovoxxel. Bilateral filter is an inbuilt plugin on*Fiji*. The Bilateral Filter has been included in *Fiji* under Plugin>Process>Bilateral Filter.

2.3 Methodology

In this paper, the general mathematical and experimental methodology of bilateral filter for denoising of ultrasound kidney image is explained. The mathematical analysis of bilateral filter is determined by equations (3) and (4) for ultrasound kidney images. The filtering process with required parameter selection step for ultrasound kidney image is shown in Figure 1.

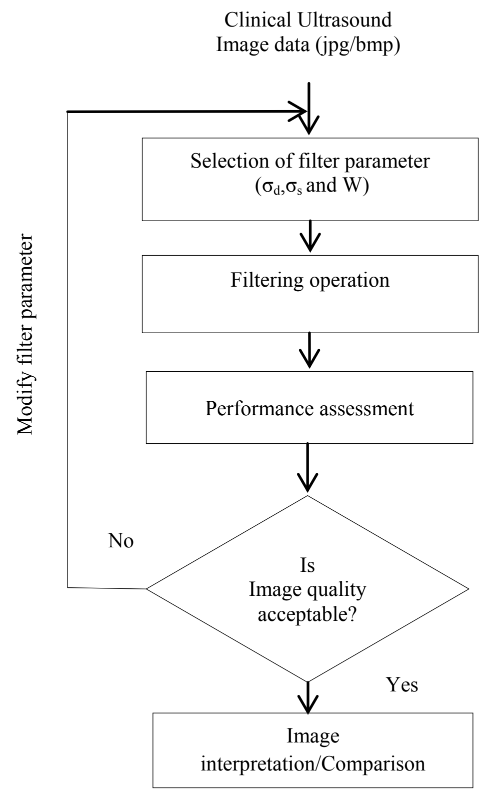

Figure 1. Filtering Process.

3. Performance Evaluation

The performance of the bilateral filter is analyzed using metrics of RMSE, SNR, PSNR and MAE. $i(x, y)$ is the image data obtained from radiology center. $I(x, y)$is denoised image then, RMSE, SNR, PSNR and MAE are given by equations (5), (6), (7) and (8) respectively.

$$RMSE=\sqrt{\frac{\sum(i(x,y)-I(x,y))^2}{MN}} \qquad (5)$$

$$SNR=10\log_{10}\left(\frac{\sum[i(x,y)]^2}{\sum[i(x,y)-I(x,y)]^2}\right) \qquad (6)$$

$$PSNR = 20\log_{10}\frac{255}{RMSE}dB \quad (7)$$

$$MAE = \frac{1}{MN}\sum|i(x,y) - I(x,y)| \quad (8)$$

The SSIM is an image quality metric correlated to the human sensory system of vision. It can be used as a benchmark to measure the image quality. The SSIM quantifies the similarity measurement of two images by luminance, contrast and structural details. The light reflecting properties of two images is determined by the mean of the intensity of pixels in the image, the contrast is determined by the standard deviation of image and the structure is determined by the correlation between two images. The SSIM is given by

$$SSIM(fi, I) = \frac{(2\mu_i\mu_I + C_1)*(2\sigma_{iI} + C_2)}{(\mu_i^2 + \mu_I^2 + C_1)*(\sigma_i^2 + \sigma_I^2 + C_2)} \quad (9)$$

Here, μ_i, is a mean and σ_i, is the standard deviation of the original image. Next, μ_I is a mean and σ_I, is the standard deviation of noise-free image and σ_{iI} is the co-variance between the original and de-noised image over a window. The constants $C_{1,}$ C_2 and C_3 are related by $C_3 = C_2/2$.

The mean SSIM is an average of all local windows. The window is moved through the image taking one pixel at a time. The SSIM values lie between *-1* to *1*. A *-1* indicate poor and a *1* indicates good similarity, respectively for original and despeckled images.

4. Results and Discussion

To evaluate the performance of the bilateral filter, a set of ultrasound kidney images are tested. The images are taken from Voluson E8 GE healthcare ultrasound machines in JPEG and BMP compressed formats. The database consist of 30 ultrasound images, each with single or multiple stones. The bilateral filtering, anisotropic, nonlocal mean and median filtering is applied on ultrasound images to process the speckle noise. Subsequently, performance measures are obtained.

From the database of 30 ultrasound stone images, Figures 2 to 8 show that eight selected sample ultrasound images are processed with bilateral filters using *Fiji* platform. The median, anisotropic, nonlocal mean and bilateral filter plugins are provided on *Fiji* software for analyzing performance. The median filter is implemented with a square window of radius 2 and can work on 8 bit gray or color images. The 2-D anisotropic filter uses default values with number of iteration 20, mask of 3×3, smoothing per iteration 1, diffusion limiter along minimal and maximal variations of 0.50 and 0.90 respectively, time step 20.0 s and edge thresholding height 5.0. The nonlocal mean filter is available as a plugin developed

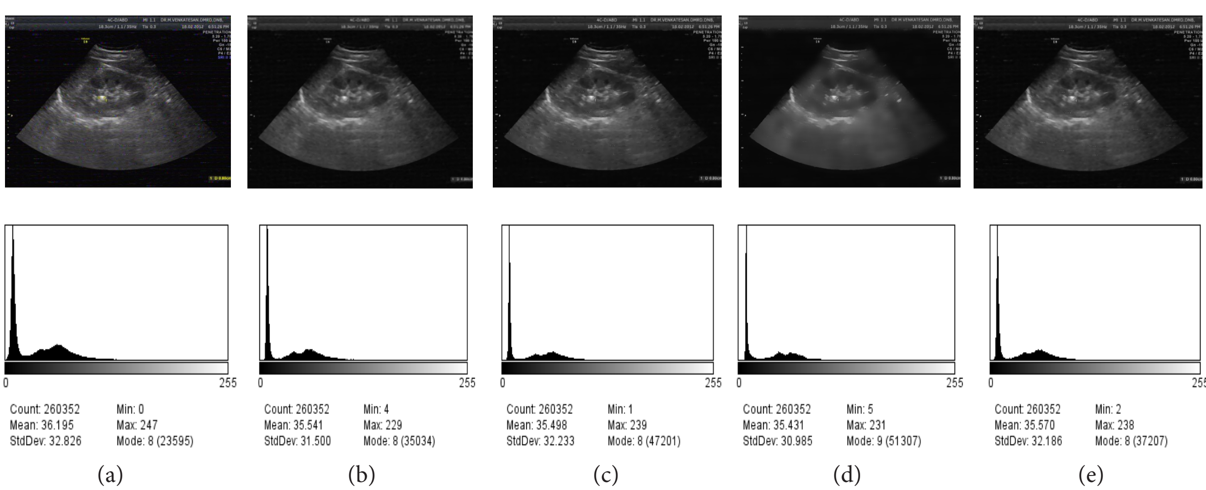

Figure 2. Sample image 1: Speckle filtering and histogram analysis. (a) Original compressed ultrasound kidney image. (b) Denoised image after median filter. (c) Denoised image after anisotropic filter. (d) Denoised image after NLM filter. (e) Denoised image after bilateral filter.

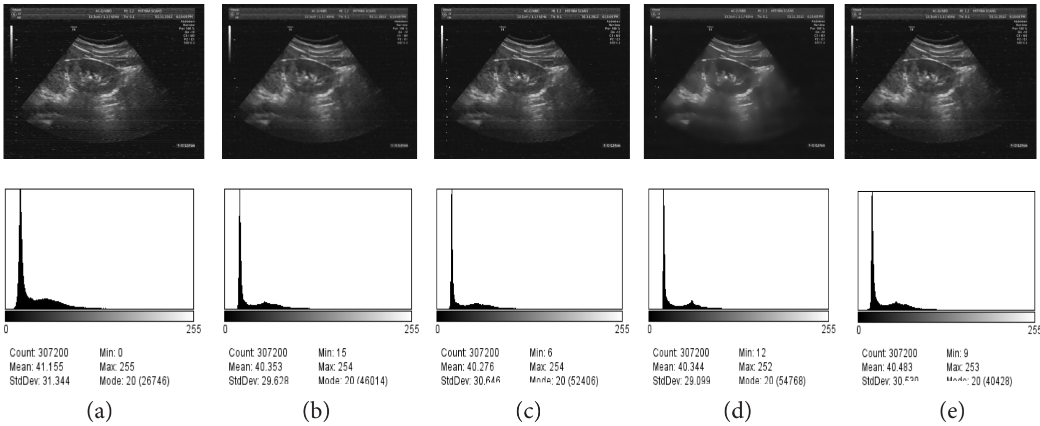

Figure 3. Sample image 2: Speckle filtering and histogram analysis. (a) Original compressed ultrasound kidney image. (b) Denoised image after median filter. (c) Denoised image after anisotropic filter. (d) Denoised image after NLM filter. (e) Denoised image after bilateral filter.

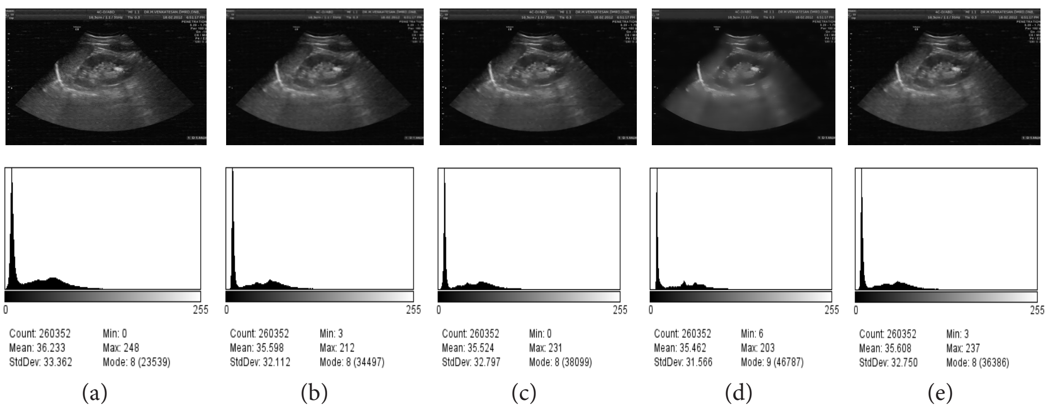

Figure 4. Sample image 3: Speckle filtering and histogram analysis. (a) Original compressed ultrasound kidney image. (b) Denoised image after median filter. (c) Denoised image after anisotropic filter. (d) Denoised image after NLM filter. (e) Denoised image after bilateral filter.

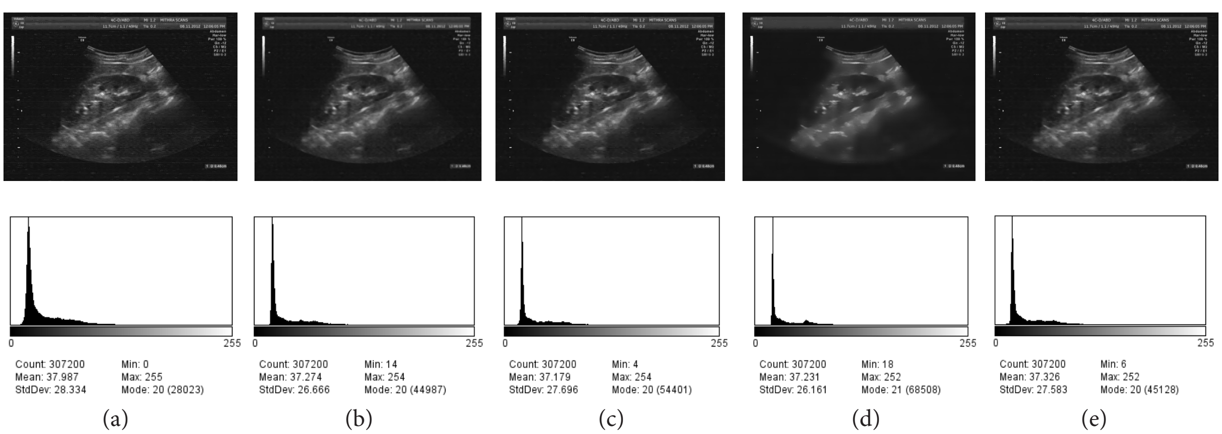

Figure 5. Sample image 4: Speckle filtering and histogram analysis. (a) Original compressed ultrasound kidney image. (b) Denoised image after median filter. (c) Denoised image after anisotropic filter. (d) Denoised image after NLM filter. (e) Denoised image after bilateral filter.

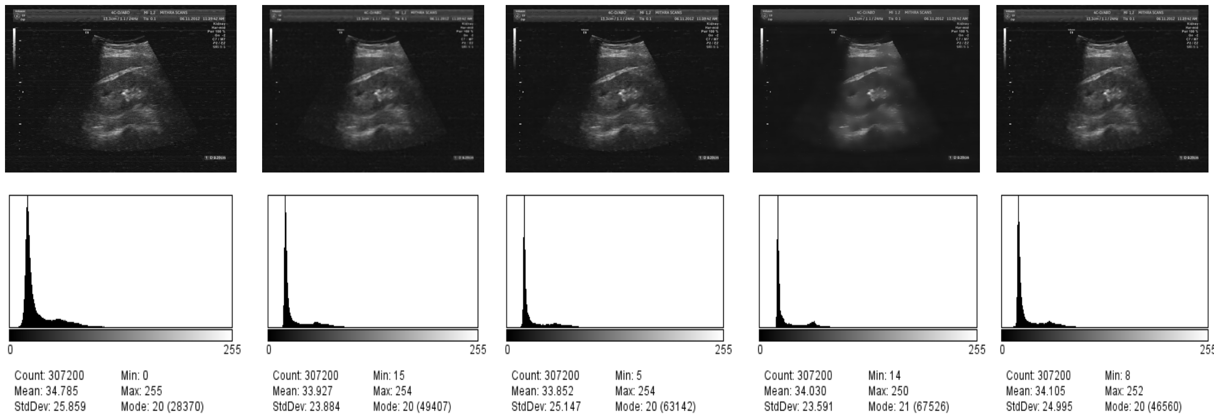

Figure 6. Sample image 5: Speckle filtering and histogram analysis. (a) Original compressed ultrasound kidney image. (b) Denoised image after median filter. (c) Denoised image after anisotropic filter. (d) Denoised image after NLM filter. (e) Denoised image after bilateral filter.

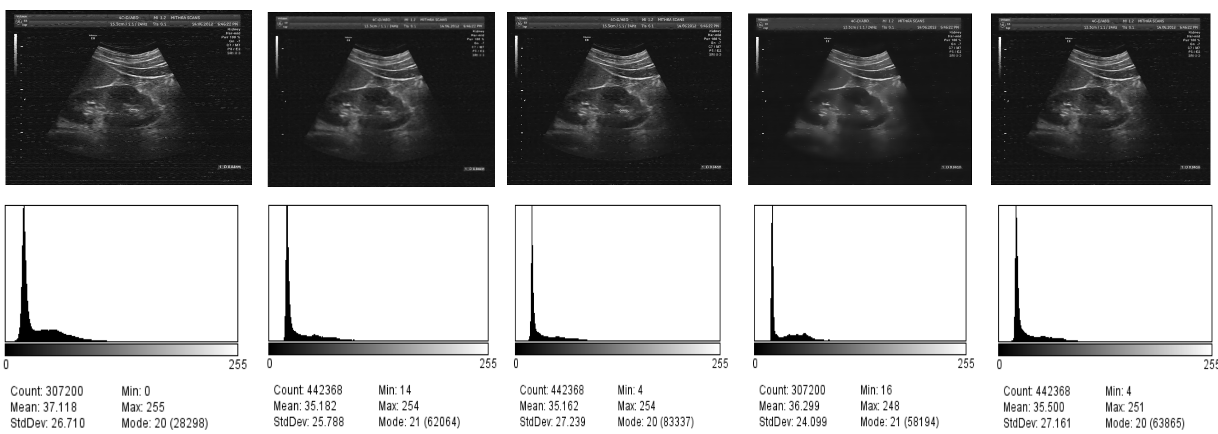

Figure 7. Sample image 6: Speckle filtering and histogram analysis. (a) Original compressed ultrasound kidney image. (b) Denoised image after median filter. (c) Denoised image after anisotropic filter. (d) Denoised image after NLM filter. (e) Denoised image after bilateral filter.

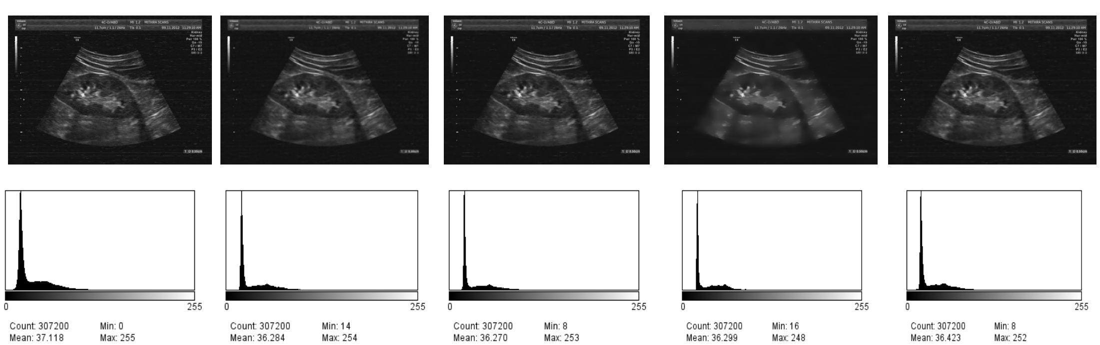

Figure 8. Sample image 7: Speckle filtering and histogram analysis. (a) Original compressed ultrasound kidney image. (b) Denoised image after median filter. (c) Denoised image after anisotropic filter. (d) Denoised image after NLM filter. (e) Denoised image after bilateral filter.

by Biomedical Imaging Group. This filter is numerically optimized one and is a multi-threaded. It works for all type of images, RGB, 8-bit, 16-bit and 32-bit. Here the default sigma value used for NLM filter is 5. The bilateral filter uses spatial radius 3 and range radius 50. The histogram of the original image and processed image is computed for analysis of filtered image for statistical qualities. The histogram reports the pixel count, minimum, maximum, mean, mode and standard deviation of original and filtered images.

Table 1 shows the values of RMSE for Figures 2 to 8 for the original image and filtered images. The RMSE values indicate the similarity and smoothing between original and filtered images. The low RMSE value indicates less blurring after filtering and maintains high similarity index. The high value of RMSE indicates over-smoothing of filtered images. The over smoothing can eliminate useful details and can cause lack of similarity in filtered images. For the simulated results, the bilateral filter yields the lesser value and the anisotropic filter has slightly higher values compared to bilateral filter. The Median and NLM filters have closer RMSE values, but higher than the bilateral filter.

Table 2 and Table 3 shows the SNR and PSNR values of images shown in Figures 2 to 8, determined for the original image and filtered image. Both SNR and PSNR indicate speckle reduction for each filtering operation. The ability of the filter to reduce the speckle noise is directly indicated by measured values. The SNR is the ratio of signal power to noise power. The PSNR is the ratio of the square of the peak value in the image to the mean square error. Both measurements should have a high value for good reconstruction. The results shown in Table 2 and Table 3 indicate that the bilateral filter has high SNR and PSNR values.

Table 4 presents the values of MAE for images shown in Figures 2 to 8. It measures the mean error. The smaller MAE value, the better is the result. It represents details of preserving restoration. Based on MAE performance bilateral filter, anisotropic filter and median filter exhibits approximately similar results. The median filter produces slightly smaller MAE compared to bilateral filter

Table 1. Comparison of RMSE values

Sample Figure	Median Filter	SRAD Filter	NLM Filter	Bilateral Filter
Figure 2(a)	4.70992	3.788801	6.509181	3.394514
Figure 3(a)	6.174806	4.528315	7.115977	3.898266
Figure 4(a)	4.590797	3.875901	6.41049	3.329347
Figure 5(a)	5.123247	3.888307	6.460781	3.537975
Figure 6(a)	5.994925	4.24072	6.676385	3.81318
Figure 7(a)	7.11658	4.961934	7.506836	4.334017
Figure 8(a)	5.604236	3.988963	7.063978	3.8263

Table 2. Comparison of SNR values

Sample Figure	Median Filter	SRAD Filter	NLM Filter	Bilateral Filter
Figure 2(a)	19.89062	21.78085	17.08036	22.73534
Figure 3(a)	17.96223	20.65596	16.73	21.75726
Figure 4(a)	20.21332	21.68362	17.31325	23.00389
Figure 5(a)	18.69538	21.09108	16.68059	21.91119
Figure 6(a)	16.45311	19.45999	15.51796	20.38304
Figure 7(a)	15.50841	18.64082	15.0447	19.81603
Figure 8(a)	17.48138	20.43	15.47072	20.79613

Table 3. Comparison of PSNR values

Sample Figure	Median Filter	SRAD Filter	NLM Filter	Bilateral Filter
Figure 2(a)	34.39366	36.2839	31.58341	37.23838
Figure 3(a)	32.31833	35.01207	31.08611	36.31337
Figure 4(a)	34.65127	36.12157	31.7512	37.44185
Figure 5(a)	33.93918	36.33595	31.92521	37.1557
Figure 6(a)	32.57512	35.58201	31.63997	36.50505
Figure 7(a)	31.08537	34.21778	30.62166	35.39298
Figure 8(a)	33.16047	36.1136	31.14981	36.47522

Table 4. Comparison of MAE values

Sample Figure	Median Filter	SRAD Filter	NLM Filter	Bilateral Filter
Figure 2(a)	1.945097	2.120502	3.869292	2.10056
Figure 3(a)	2.675537	2.340345	4.143079	2.401764
Figure 4(a)	1.917815	2.205702	3.809408	2.061923
Figure 5(a)	2.195768	2.130556	3.729166	2.154892
Figure 6(a)	2.574114	2.204625	3.791318	2.359352
Figure 7(a)	3.177562	2.647894	4.346019	2.743516
Figure 8(a)	2.464749	2.107272	4.11386	2.33788

for images shown in Figures 4 and 6. All other values of median and anisotropic images are higher than that of the bilateral filter. This analysis indicates that the bilateral filter has a good edge preserving capability.

Table 5 is listed with SSIM values of images shown in Figures 2 to 8 for different filters. The value closer to 1 indicates the structural preservation in filtered images. From results, the bilateral filter produces values closure to 1, indicating better performance. Figure 9 shows the graphical representation of RMSE, SNR, PSNR and SSIM of the tested filters. The results summary conclusively indicates that the performance of the bilateral filter is more suitable for speckle noise reduction in kidney ultrasound images compare to any other filter test.

Table 5. The performance of filters based on SSIM values

Sample Figure	Median Filter	SRAD Filter	NLM Filter	Bilateral Filter
Figure 2(a)	0.8366	0.884	0.7896	0.9048
Figure 3(a)	0.7759	0.8542	0.7581	0.8828
Figure 4(a)	0.8421	0.8745	0.7949	0.9059
Figure 5(a)	0.8107	0.8641	0.7832	0.889
Figure 6(a)	0.7716	0.8584	0.754	0.8752
Figure 7(a)	0.8426	0.9149	0.8018	0.9588
Figure 8(a)	0.7909	0.8715	0.7561	0.8841

5. Conclusion

This paper has presented an analysis on the performance of four different types of filters applied on ultrasound kidney images with speckle noise. Simulation tests are performed using an open source software tool Fiji. The performance of bilateral filter for reducing speckle noise in kidney ultrasound image is better than any other filter. Even though the same filter is already applied for general ultrasound images, but in this research study, it is particularly applied to kidney images with the presence of stones. The ultrasound images of various organs differ from each other due to the fact that its acquisition requires different frequency range depending upon location and depth in the body. The analysis on the performance of the bilateral filter can be helpful for developing an automatic stone

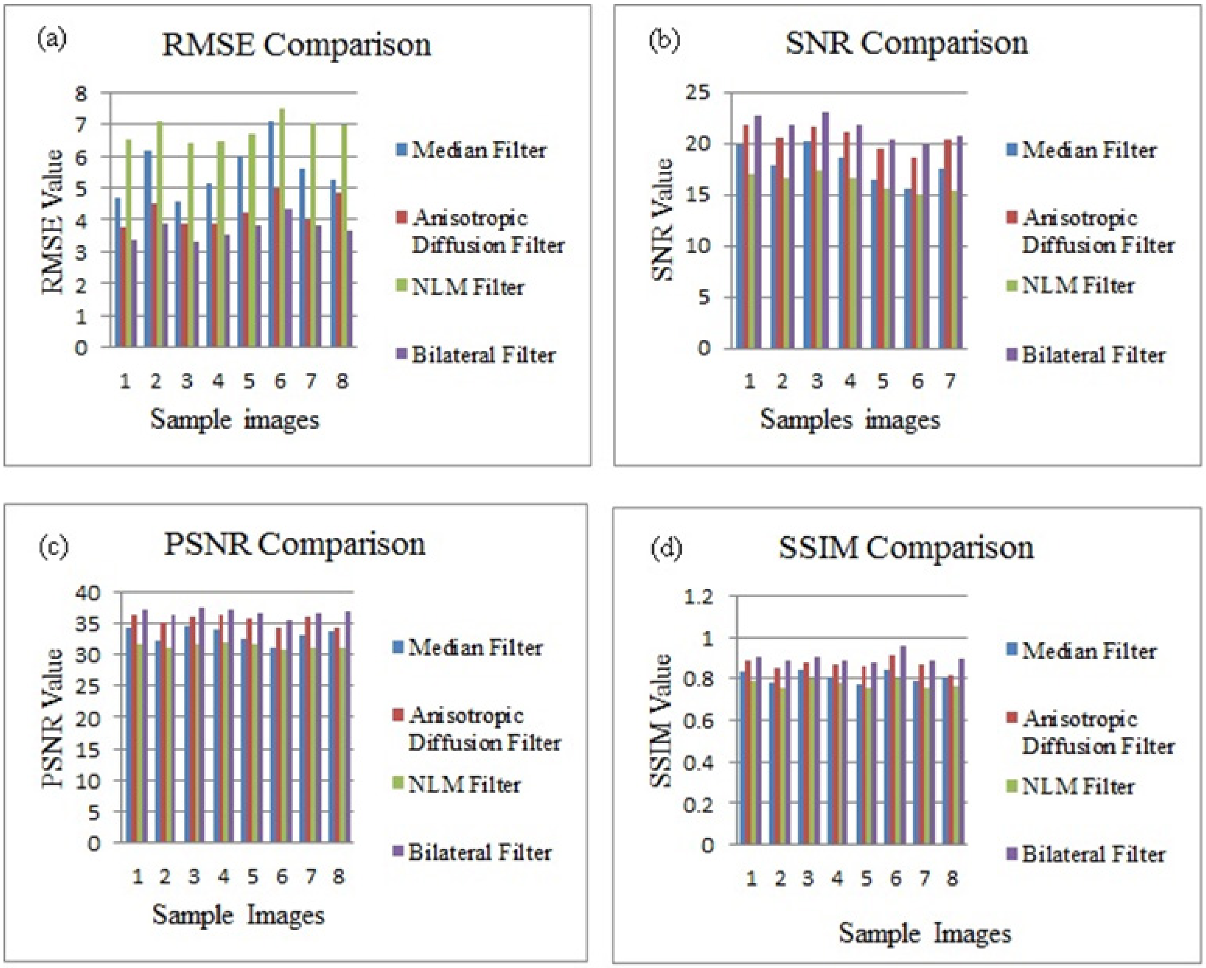

Figure 9. Comparison of (a) RMSE (b) SNR (c) PSNR (d) SSIM values of Median, Anisotropic Diffusion Filter and Bilateral Filter.

detection system. The noise reduction increases the probability of the correct diagnosis of stones presence in kidney images.

The future work may concentrate on improving the performance of the bilateral filter by means of hybridization or by replacing filter kernels. New architecture of filter can also be an area for further research. This can be useful for performing better segmentation of images of kidney with stones.

6. Acknowledgements

The authors sincerely acknowledge the contribution and help extended by Dr. P.Venkatesan, Professor, Salem, Tamil Nadu, India for providing different and actual ultrasound B-scan images for carrying out simulation tests under this research study.

7. References

1. Eltoft T. Modeling the amplitude statistics of ultrasonic images. IEEE Transaction on Medical Imaging. 2006 Feb; 25(2):229–40.
2. Tomasi C, Manduchi R. Bilateral filter for gray and color images. Proceedings of 6th International Conference on Computer Vision; Bombay. 1998 Jan 4–7. p. 839–46.
3. Bhonsle D, Chandra V, Sinha GR. Medical Image Denoising Using Bilateral Filter. I J Image, Graphics and Signal/ processing. 2012 Jul; 4(6):36–43.
4. Balocco S, Gatta C, Pujol O, Mauri J, Radeva P. SRBF: Speckle Reducing Bilateral Filtering. Ultrasound in Medicine and Biology. 2010 Aug; 36(8):1353–63.
5. Tang J, Guo S, Sun Q, Deng Y, Zhou D. Speckle reducing bilateral filter for cattle follicle segmentation. International Conference on Bioinformatics and Computational Biology. Las Vegas, NV, USA. 2010 Nov; 11(2):S9.

6. Zhang M, Gunturk BK. Multiresolution bilateral filtering for image denoising. IEEE Transaction on Image Processing. 2008 Dec; 17(12):2324–33.
7. Raj VNP, Venkateswarlu T. Ultrasound medial image denoising using hybrid bilateral filtering. International Journal of Computer Applications. 2012 Oct; 56(14): 44–51.
8. Wenxuan SHI, Jie LI, Minyuan WU. An image denoising method based on multiscale wavelet thresholding and bilateral filtering. Wuhan University Journal of Natural Science. 2010 Apr; 15(2):148–52.
9. Kao WC, Chen YJ. Multistage noise filtering and edge detection for color image enhancement. IEEE Transaction on Consumer Electronics. 2005 Nov; 51(4):1346–51.
10. Han JW, Kim JH, Cheon SH, Kim JO, Ko SJ. A novel image interpolation method using the bilateral filter. IEEE Transaction on Consumer Electronics. 2010 Feb; 56(1):175–81.
11. Loganayagi T. De-noising methods for ultrasound renal images – A comparative study. Int J of Appl Engg Research. 2015; 10(4):8741–56.
12. Anitha U, Malarkkan S. A novel approach for despeckling of sonar image. Indian Journal of Science and Technology. 2015 May; 8(S9):252–9.
13. Saini K, Dewal ML, Rohit M. A modified hybrid filter for electrocardiographic image noise removal. I J Signal Processing, Video Processing and Pattern Recognition. 2012 Jun; 5(2):61–72.
14. Michailovich OV, Tannenbaum A. Despeckling of ultrasound images. IEEE Transaction on Ultrosonics. Ferroelectrics and Frequency Control. 2006 Jan; 53(1):64–78.
15. Gupta A, Gosain B, Kaushal S. A comparison of two algorithms for automated stone detection in clinical B-mode ultrasound images of the abdomen. Journal of clinical monitoring and computing. 2010 Oct.; 24(5):341–62.
16. Buades A, Coll B, Morel JM. A non-local algorithm for image denoising. IEEE Computer society conference on Computer Vision and Pattern Recognition. San Diego, California. 2005 Jun 20-25; 2:60–5.
17. Shreyamsha Kumar BK. Image denoising based on non-local mean filter and its method noise. Signal, Image and Video Processing. 2013 Nov; 7(6):1211–27.
18. Schindelin J, Arganda-Carreras I, Frise E, et al. Fiji: an open-source platform for biological-image analysis. Nature methods. 2012 Jun; 9(7):676–82.
19. Hore A, Ziou D. Image Quality metrics: PSNR vs. SSIM. 20th International Conference on Pattern Recognition. Istanbul. 2010 Aug 23-26; 2366–9.